Food Chemistry 345 (2021) 128778

Contents lists available at ScienceDirect

Food Chemistry

journal homepage: www.elsevier.com/locate/foodchem

NMR-based metabolomic study of Apulian Coratina extra virgin olive oil extracted with a combined ultrasound and thermal conditioning process in an industrial setting

L. Del Coco [a], C.R. Girelli [a], F. Angilè [a], I. Mascio [b], C. Montemurro [b,c], E. Distaso [d], P. Tamburrano [d], S. Chiurlia [g], M.L. Clodoveo [e], F. Corbo [f], R. Amirante [d], F.P. Schena [g,h], F. P. Fanizzi [a,i,*]

[a] Department of Biological and Environmental Sciences and Technologies, University of Salento, 73100 Lecce, Italy
[b] Department of Soil, Plant and Food Sciences, Section of Genetics and Breeding, University of Bari Aldo Moro, via Amendola 165/A, 70125 Bari, Italy
[c] Spin off Sinagri s.r.l., University of Bari Aldo Moro, via Amendola 165/A, 70125 Bari, Italy
[d] Department of Mechanics, Mathematics and Management (DMMM), Polytechnic University of Bari, Via Orabona 4, Italy
[e] Interdisciplinary Department of Medicine, University of Bari Aldo Moro, 70125 Bari, Italy
[f] Department of Pharmacy-Pharmaceutical Sciences, University of Bari Aldo Moro, 70125 Bari, Italy
[g] Schena Foundation, European Center for the Study of Renal Diseases, 70010 Valenzano (Ba), Italy
[h] Department of Emergency and Organ Transplantation, Renal Unit, University of Bari, 70124 Bari, Italy
[i] University of Salento Local Unit of Consorzio Interuniversitario di Ricerca in Chimica dei Metalli dei Sistemi Biologici (CIRCMSB), Via Celso Ulpiani, 27-70126 Bari, Italy

ARTICLE INFO

Keywords:
Extravergin olive oil
Coratina oil
NMR spectroscopy
Ultrasound-assisted extraction system
Polyphenols

ABSTRACT

The innovative combination of ultrasound (Us) with a thermal exchanger to produce high quality extra virgin olive oil (EVOO) was studied using Nuclear Magnetic Resonance (NMR) spectroscopy and multivariate analysis (MVA). Major and minor metabolomic components of Apulian Coratina EVOO obtained using the two methods were compared. Early and late olive ripening stages were also considered. An increased amount of polyphenols was found for EVOOs obtained using the Us with respect to the conventional method for both early and late ripening stages (900.8 ± 10.3 and 571.9 ± 9.9 mg/kg versus 645.1 ± 9.3 and 440.8 ± 10.4 mg/kg). NMR spectroscopy showed a significant increase ($P < 0.05$) in polyunsaturated fatty acids (PUFA) as well as in the tyrosol and hydroxytyrosol derivatives, such as oleocanthal, oleacein, and elenolic acid, for both ripening stages. In conclusion, NMR spectroscopy provides information about the metabolomic components of EVOOs to producers, while the Us process increases the levels of healthy bioactive components.

1. Introduction

Italy has the greatest number of quality extra virgin olive oil (EVOO) producers in Europe according to UNAPROL (Consorzio Olivicolo Italiano) and the Institute of Services for the Agricultural and Food Market (ISMEA), as reported by the Olive Oil Times (Olive Oil Times, 2020). Puglia is the largest producer of olive oil in Italy, despite climate issues and areas affected by *Xylella fastidiosa*; Calabria and Sicily are the second and third largest producers, respectively (Olive Oil Times, 2020). The European Union (EU) provides rigorous marketing standards for olive oil in the EU market (Conte et al., 2019).

These marketing standards are based on the EU regulations (European Commission Regulation 2568/91). The standards are used because olive oil, compared with other food products, is at risk of fraud because of its high economic value. The chemical and sensory features of extra virgin olive oil (EVOO) can be attributed mainly to its fatty acid content, particularly oleic acid and polyphenol compounds (Bellumori, Cecchi, Innocenti, Clodoveo, Corbo, & Mulinacci, 2019). The major polyphenol compounds are tyrosol and hydroxytyrosol and its derivatives, such as oleuropein complex; these compounds contribute to the quality of EVOO because they are associated with the health claims approved by the European Food Safety Authority (EFSA) (European Commission Regulation 432, 2012; Bellumori, Cecchi, Innocenti, Clodoveo, Corbo, & Mulinacci, 2019; Conte et al., 2019). Currently, there is

* Corresponding author at: Department of Biological and Environmental Sciences and Technologies, University of Salento, 73100 Lecce, Italy.
E-mail address: fp.fanizzi@unisalento.it (F.P. Fanizzi).

https://doi.org/10.1016/j.foodchem.2020.128778
Received 16 June 2020; Received in revised form 26 November 2020; Accepted 28 November 2020
Available online 3 December 2020

no official method for measuring all free and linked forms derived from secoiridoid structures of tyrosol and hydroxytyrosol (Bellumori, Cecchi, Innocenti, Clodoveo, Corbo, & Mulinacci, 2019), although the organoleptic and nutritional value of these compounds are widely known. It has been demonstrated that several classes of phenolic molecules are responsible for the multiple pharmacological properties of EVOO (Olmo-Cunillera et al., 2019), as well as the antioxidant properties, which prevent and manage many types of cardiovascular pathologies (Reboredo-Rodríguez et al., 2018) and cancer. The antioxidant properties of EVOO are mainly associated with tyrosol, which prevent damage from reactive oxygen species (ROS). Hydroxytyrosol and its derivatives, including oleuropein (3,4-DHPEA) and the elenolic acid glucoside, have anti-tumor activity, while oleocanthal, has anti-proliferative effects on cancer cell lines and similar pharmacological activity as ibuprofen (Reboredo-Rodríguez et al., 2018). In terms of the organoleptic properties, the bioactive phenolic molecules are also responsible for the bitterness and pungent taste of EVOO, which is mainly attributed to oleuropein aglycon (Arafat, Abd-Elfatah, & Aml, 2020). The organoleptic properties have a wide impact on characterizing high quality EVOOs for the EU marketing standards (European Commission Regulation 29, 2012). A sensory analysis showed that, among the Italian cultivars, the Coratina cultivar has a high bitterness and a very strong pungency (Del Coco, De Pascali, & Fanizzi, 2014). Due to the presence of clonal variations and misnaming of the Coratina genotypes, it is important to define the genetic identity of trees in order to minimize the influence of genotype effect (D'Agostino et al., 2018). It is also useful to study the effect that the extractability processes developed for use in the olive oil sector have on the molecular profiles of the Coratina EVOO. Many innovative processes have been developed to increase yields and improve quality without creating additional energy costs (Amirante & Clodoveo, 2017). These processes include the application of ultrasound (Us), microwaves, pulsed electric fields, and Us combined with a heat exchanger (Clodoveo, 2019). The Us method focuses on improving the malaxation stage during the olive oil extraction process. This method was originally developed in the laboratory and adapted for industrial commercial use. It is based on avoiding undesired temperature increases in the olive paste and on improving the extractability of minor compounds without causing changes in the quality indices (Amirante & Clodoveo, 2017; Clodoveo, 2019). Few studies have been published on the enrichment of phenolic compounds in olive oil using Us-assisted extraction technology on phenols from olive mill wastewater (Jerman Klen & Mozetič Vodopivec, 2011).

It is well known that NMR spectroscopy is particularly suitable for the investigation of complex matrices such as EVOO (Girelli, Del Coco, & Fanizzi, 2017; Girelli, Del Coco, Papadia, De Pascali, & Fanizzi, 2016; Girelli et al., 2018; Olmo-Cunillera et al., 2019). In particular, the NMR-based metabolomic approach allows a comprehensive EVOO characterization at different steps of the olive harvesting season. This includes the efficiency evaluation for the ultrasound extraction of polyphenols in comparison with the traditional oil extraction process. In this study, the ultrasound technology has been tested in an industrial olive mill, and the metabolomic profile of the produced oils has been determined and analysed by a NMR-based chemometric approach.

2. Materials and methods

2.1. Sample selection, DNA extraction and molecular characterization

A microsatellite marker (SSR) analysis was conducted to verify genetic matching in Coratina samples used for the study. Fifty young leaves were collected along the canopy, from 65 trees distributed in the four different fields: A (10 trees, samples 1A-10A), B (25 trees, samples 11B-35B) and C (20 trees, samples 36C–55C) selected from a homogenous pedoclimatic region of Bari province (South Italy). Because of the presence of genetic diversity trees in the A field, other 10 leave samples were collected in the D field (samples 1D-10D). All the samples were compared with the Coratina certified genetic profile provided by the private database of the Department of Soil, Plant and Food Sciences, University of Bari Aldo Moro. The leaf samples were lyophilized and the total genomic DNA was extracted from 50 mg of tissue (Spadoni et al., 2019). DNA was checked for its quality and quantity using the NanoDropTM ND2000C (Thermo Fisher Scientific, Waltham, MA, USA), and normalized at 50 ng/ml into a 96-well plate (Nunc 96-Well Multiwell Plates). A set of 11 nuclear SSRs was used: DCA03, DCA05, DCA09, DCA15, DCA16, DCA17, DCA18 (Sefc, Lopes, Mendonça, Santos, Machado, & Machado, 2000), GAPU71b, GAPU101 (Carriero, Fontanazza, Cellini, & Giorio, 2002), EMO90, EMOL (De la Rosa, James, & Tobutt, 2002) and UDO28 (Cipriani, Marrazzo, Marconi, Cimato, & Testolin, 2002). This set was selected among those available in literature, due to the proven suitability and reliability for olive cultivar's discrimination (Sion et al., 2019; Boucheffa et al., 2017). Primers pairs were synthesized by Thermo Fisher Scientific (MA, USA) and each forward primer was labelled with one of the following dyes: 6FAM™, NED™, VIC® and PET™. The amplification reactions were carried out in a final volume of 12.5 µl, containing 30 ng of genomic DNA, 1X DreamTaq buffer, 0.2 mM of each dNTP, 0.25 µM of each forward and reverse primer, 1U DreamTaq DNA polymerase (Thermo Fisher Scientific), using T100 thermal cycler (Bio-Rad Laboratories, Hercules, CA). The amplification protocol was performed according to di Rienzo et al., 2018. Two µL of PCR products were added to 0.5 µl of GeneScan™ – 600 LIZ® Size Standard (Applied Biosystem, USA) and 9.5 µl of Hi – Di Formamide (Applied Biosystem, USA) and separated by capillary electrophoresysis using an automatic sequencer ABI PRISM 3100 Avant Genetic Analyzer (Applied Biosystems, USA). Detection, sizing and data collection were carried out using the GeneMapper® genotyping software v.5 (Applied Biosystems, USA).

2.2. Extra virgin olive oil extraction process by the ultrasound system

The proposed ultrasound system applied to the EVOO extraction process is shown in Fig. 2S. Aim of our study has been to demonstrate that the newest set-up represents an actual step forward in obtaining a continuous process, as well as in increasing yield and quality (increasing phenols) concurrently. Schematically, the left hand of the Fig. 2S shows the typical so-called "continuous" process where the harvested olives are withdrawn from the plants, dropped into a hopper and laid down onto a conveyor belt that carries olives to the washing machine. The vibrating machine removes leaves and other debris to protect the extraction plant and to avoid the off-flavours deriving from the presence of foreign bodies. After that, the olives are washed to remove soil or other residues and so the pre-process stage is completed. Then, another conveyor belt carries the olives to the crushing phase which consists of the extraction process. The crushing phase breaks the olive fruit tissue by means of a strong mechanical action. The break process of the vegetal cells produces the release of oil, as well as heat due to energy dissipation. Next, the olive paste moves to a piping and an upstream mono pump. Malaxation represents the subsequent step and it consists of a usual cylindrical tank equipped with a shaft with rotating arms and stainless steel blades, while in the new concept of the proposed layout, the Us treatment is applied by means of the sono-heat-exchanger (SHE).

During the malaxation phase the olive paste is continuously agitated at controlled temperature to help the small droplets of the oil formed during the milling to merge into large drops (coalescence phenomenon), allowing an easier separation through a centrifugal system. Once the malaxing process has been completed, the paste is removed from the bottom of the tank by another pump which feeds the paste into a horizontal centrifuge to separate the oily phase from the solid and liquid phases of the olive paste. Water can be (or not) added to dilute the incoming paste according to the Stokes law to divide extracted oil from vegetation water and solids (olive pomace). Finally, a vertical centrifuge allows clarifying the extracted oily phase by adding lukewarm tap water. In this way, the equipment separates the residual water and the solid

impurities in order to obtain clear oil. The SHE, previously described by Amirante and Clodoveo (2017) is placed between the crusher and the decanter and it replaces the malaxer. During the olive past transit, the ultrasound effect occurs and, by means of cavitation, the device breaks the cell left intact in the first crushing process. The present device is designed as an octagonal cross section equipped with plate style transducer, each of 100 W of power and 23 kHz of frequency. The shape ensures the continuous and best adhesion between the paste and the transducers, thus improving the performance of the ultrasound machine prototype used by Clodoveo et al., 2017. This SHE avoids air bubbles formation or flux separation phenomena which worsen the ultrasound transmission. Moreover, it encases the ultrasound and the heat exchange processes; then, it can be scaled, according to the plant size, in a more flexible way due to its modular structure. The SHE, employing the plate shape transducers, is composed of a couple of annular sections (Amirante & Clodoveo, 2017). The olive paste flows into the external annular section, while cold or hot water flows in the internal annular section to control temperature inside the olive paste. Outside the external annular flow section, a transducer for each side of an octagonal shape is set-up to provide ultrasounds. The energy per kilogram of olive paste is due to the power of each transducer and the flowrate flowing inside the SHE. The choose of this couple of parameters should be performed keeping in mind that the best results can be achieved using 15 ÷ 18 kJ/kg at 20 ÷ 30 kHz (Clodoveo et al., 2015, 2017). Since the flow rate of the oil miller is around 900 kg/h, the maximum value of the power to apply is 4 kW, in correspondence of 15 kJ/kg. To assure the right range of specific energy (15 kJ/kg), the SHE is equipped with a flow meter which can measure the value of flow rate in each work condition of the miller and a Programmable Logic Controller (PLC) can calculate in real time the appropriate power value. The latter power value is transmitted from PLC to the digital driver of the Ultrasound transducers. The driver set this power value at the Us transducers. The frequency value chosen for the SHE (2019 version) is approximately 23 kHz. This frequency value is automatically controlled by the digital driver to assure the best resonance value. The resonance frequency is not a constant value because it changes due to some variables as the olive paste rheological parameters, which are dependent on olive cultivar, olive- ripening and, the management of the olive grove. Thus, the provided frequency value is chosen by the driver in the first seconds of the working time, during which the best value for the resonance is measured. This tuning action is very important to obtain the right vibration of the Us transducer.

Another fundamental parameter is the pressure value inside the SHE that is the result of the continuous loss loads of the pipes downstream the SHE. This value must be in a range of 1 to 5 bar (manometric pressure). High pressure values are not suitable for the cavitation phenomenon and can damage the SHE, while lower values can reduce the Us exchange between transducers and olive paste. A pressure transducer is present in the SHE to check the pressure value by means of the PLC.

In order to obtain the best quality, recent evidences suggest that it is crucial to keep the olive paste temperature in the range of 20 ÷ 25 °C (depending on the olive cultivar and fruit maturity index). This can be achieved by employing a heat exchanger, which can be integrated in the ultrasound device. A cold-water flow (4 ÷ 5 °C) can be provided into the inner annular space to decrease the olive paste temperature in the geographical areas characterized by a high ambient temperature. On the other hand, a warm water flow (20 ÷ 50 °C) can be provided into the inner annular space to warm up the olive paste in geographical areas characterized by low temperature during the harvesting season. Two thermistors are set in the SHE to control the working temperatures.

2.3. Olive sampling and EVOO extraction

Sixty Coratina extra virgin olive oil samples were obtained from 55 olive trees located in the B, C and D fields in two different ripening stages of the 2019/2020 olive harvesting campaign, in particular in the months of November 2019 (I) and January 2020 (II). Oils were sampled at regular intervals within the continuous milling process and sequentially separated during the continuous system of extraction. The olive oil samples were stored in sealed dark glass bottles at room temperature in the dark prior to laboratory analysis.

2.4. Analytical parameters

Determination of oil quality parameters as acidity value, peroxide value and UV absorption (K_{270} and K_{232}) and total phenolic content were carried out according to the analytical methods described in Regulation EEC/2568/91 and next amendments and additions by Giuseppe Vacca Olii S.r.l. – Bitonto, Italy (Commission Regulation, 1991; Regulation, 2016).

2.5. Sample preparation for ^{1}H NMR analysis and data processing

NMR samples were prepared dissolving ~ 140 mg of olive oil in $CDCl_3$ and adjusting ratio of olive oil: $CDCl_3$ to 13.5: 86.5 (% w/w). This ratio was chosen to give the best trade-off for sensitivity/solution viscosity in spectral acquisition (Bruker Italia, standardized procedure for olive oil) (Girelli et al., 2018; Girelli, Del Coco & Fanizzi, 2017). Then, 600 μl of the prepared mixture were transferred into a 5-mm NMR tube. ^{1}H NMR spectra were recorded on the Bruker Avance spectrometer (Bruker, Ettlingen, Germany) operating at 400.13 MHz, T = 300 K, equipped with a PABBI 5-mm inverse detection probe incorporating a z axis gradient coil. NMR experiments were performed after sample randomization to avoid biasing results due to instrument conditions or operator related differences. The entire process was conducted under full automation, after loading individual samples on a Bruker Automatic Sample Changer (BACS-60), interfaced with the IconNMR software (Bruker). In order to optimize the NMR conditions, automated tuning and matching, locking and shimming and 90° hard pulse calibration P (90°) were carried out for each sample using standard Bruker routines ATMA, LOCK, TOPSHIM and PULSECAL. After a waiting period of 300 s for temperature equilibration, two ^{1}H NMR experiments were performed for each sample: the standard one-dimensional (^{1}H ZG) NMR experiment and the one-dimensional ^{1}H NOESYGPPS NMR pulse sequence, with suppression of the strong lipid signals (20 frequencies), in order to enhance the signals of the minor components present in EVOOs (Del Coco, De Pascali, & Fanizzi, 2014). Spectra were obtained by the following conditions: zg pulse program (for ^{1}H ZG), 64 K time domain, spectral width of 20.5555 ppm (8223.685 Hz), p1 (F1 channel 90° ^{1}H transmitter pulse) 12.63 μs, pl1 −1.00 db (decibel), 16 repetitions, relaxation delay (RD) and acquisition time (AQ) of 4 s and ~3.98 s, respectively, resulting in a total recycle time of ~ 7.98 s (Del Coco, De Pascali, & Fanizzi, 2014; Girelli et al., 2018); noesygpps1d.comp2 pulse program (for ^{1}H NOESYGPPS NMR) 32 K time domain, spectral width 20.5555 ppm (8223.685 Hz), p1 12.63 μs, pl1 −1.00 db, 32 repetitions. ^{1}H NMR spectra were obtained by the Fourier Transformation (FT) of the FID (Free Induction Decay), applying the exponential multiplication (EM) with a line broadening factor of 0.3 Hz, automatically phased and baseline corrected. Chemical shifts were reported with respect to the TMS (tetramethylsilane as an internal standard 0.03% v/v) signal set at 0.00 ppm, obtaining good peak alignment.

For spectra analyses, Topspin 2.1 (Bruker) and Analysis of Mixture Amix 3.9.13 (Bruker, Biospin, Italy) softwares were used for both simultaneous visual inspection and statistical bucketing process. By this last procedure (the bucketing process of 0.04 ppm width) two different matrices were obtained, the first from the ^{1}H ZG spectra (BUCKET-1, considering the entire NMR spectrum, in the range 10.00–0.5 ppm) and the second from ^{1}H NOESYGPPS (BUCKET-2 considering the range 10.00–5.5 ppm). In both cases, the spectral region between 7.60 and 6.90 ppm was discarded, because of the residual peak of chloroform presence. The total sum normalization was applied to the data to minimize small differences due to sample concentration and/or experimental conditions among samples. The Pareto scaling procedure was

applied, performed by dividing the mean-centered data by the square root of the standard deviation (van den Berg, Hoefsloot, Westerhuis, Smilde, & van der Werf, 2006). Unsupervised (principal component analysis, PCA) and supervised (partial least squares discriminant analysis, PLS-DA and orthogonal partial least squares discriminant analysis, OPLS-DA) multivariate statistical analyses were performed on both the data matrices (BUCKET-1 and BUCKET-2) using the SIMCA 14 software (Sartorius Stedim Biotech, Umeå, Sweden). OPLS-DA works by separation of the systematic variation of the data (X, i.e. the bucket reduced NMR data) into two parts, one correlated (predictive) to Y (class membership) and one part that is uncorrelated (orthogonal) to Y. The robustness of the statistical models was tested by cross-validation default method (7-fold) and further evaluated with a permutation test (20 permutations) (Bro, Kjeldahl, Smilde, & Kiers, 2008). The quality of the statistical models (in particular the total variations in the data and the internal cross-validation) was described by R^2 (the variance explained) and Q^2 (the predictive capability) parameters and probability (p[CV-ANOVA], 95.0% confidence level, obtained from the analysis of variance testing of cross-validated predictive residuals (CV-ANOVA) (Del Coco et al., 2018). In particular, for the supervised models (PLS-DA and OPLS-DA), R^2 is described by R^2X and R^2Y, which represent the fraction of variance of the X and Y matrix, respectively. Loadings describe the correlations that the considered Principal or PLS components have with the original variables (i.e. the bucket reduced NMR data). Finally, for discriminating metabolites, obtained by MVA analyses, mean values of integrals were calculated from selected ^{1}H NMR peaks areas and reported as Log_2 fold change (FC) ratio.

3. Results

3.1. Molecular characterization data

Eleven selected SSR markers were used to amplify sixty-five leaf samples collected by the four olive tree fields. In the first step 55 samples of the A, B and C fields were genotyped and compared with the Coratina variety profile. The results highlighted the complete genetic similarity among 50 analyzed samples: 1A and 5A to 8A and all samples collected in the B and C fields. In other words, the SSR profiles matched perfectly with the genetic profile of Coratina presents in the dataset. However, five samples, 2A, 3A, 4A, 9A and 10A, differed from the others. In particular, samples 2A, 3A, 4A and 9A showed 12 or 13 alleles in common with the Coratina profile and between 18 and 21 alleles in common with each other. Sample 10A showed a greater genetic diversity both with the field samples (between 7 and 9 alleles in common) and the Coratina profile (only 9 alleles in common). To replace the 5 genetically diverse samples, 10 other leave samples were collected from the D field and analyzed. The data showed that the 10 samples matched the genetic identity of all the samples with Coratina profile. These results support the importance of genotyping olive trees.

3.2. Ultrasound data

In this study, the olives were harvested by a trunk shaker machine and processed 6 h later. The maturity index was determined according to the method proposed by the International Olive Council. Three aliquots of 500 ml olive oil were obtained after each extraction and were stored in dark bottles at 15 °C. The extraction yield (EY) content was determined following our procedure (Clodoveo et al., 2017). The olive oil extraction experiments were performed in triplicate on samples obtained during November from field D and January from field C. A comparison of the EY obtained using the conventional method (Cm) and using the Us method is shown in Table 1. An increased extractability of the olive oil and biophenol quantity was observed when the sono-heat-exchanger (SHE) was employed.

Table 1
Mean ± SD of the oil extractability and bio phenols quantity using the traditional and the innovative SHE systems (I, November; II, January).

Miller	I, Cm Giovinazzo	I, Us Giovinazzo	II, Cm Sannicandro	II, Us Sannicandro
Yield (kg_{evoo}/ $100kg_{olives}$)	14.4 ± 0.1	15.6 ± 0,1	13.1 ± 0.1	13.3 ± 0.1
% yields increment	7.6 ± 0.05		1.5 ± 0,05	
Bio phenols (mg/kg)	645.1 ± 8.3	900.8 ± 4.2	440.8 ± 5.4	571.9 ± 9.2
% bio phenols increment	39.63 ± 3.1		29.74 ± 3.6	
MATURITY DEGREE	GREEN		DARK	

Abbreviations: Cm = conventional method; Us = ultrasound technique.

3.3. Comparison of oil quality indices and phenolic content of EVOOs obtained using the Ultrasound and the Conventional methods

The quantitative differences in the oil quality indices and the phenolic content of the EVOO obtained using Ultrasound technology and the conventional method are shown in Table 2. We considered two different ripening stages in our study: an early ripening (I) stage in November and a late ripening (II) stage in January. The results showed that the Coratina EVOO samples from the early ripening stage obtained using the Cm had a lower percentage of acidity value in terms of free oleic acid compared with the samples obtained using the Us method: 0.10% ± 0.03% and 0.11% ± 0.003%, respectively. The highest percentage of acidity value was found in samples from the late ripening stage obtained using the Cm: 0.35% ± 0.03% acidity. As reported by other authors (Deiana, Santona, Dettori, Culeddu, Dore, & Molinu, 2019; Olmo-Cunillera, López-Yerena, Lozano-Castellón, Tresserra-Rimbau, Vallverdú-Queralt, & Pérez, 2019), biophenols, such as oleocanthal, oleacein and aglycon of oleuropein and ligstroside were the most abundant molecules in all olive varieties, while free tyrosol and hydroxytyrosol were mainly present at low levels. Interestingly, in this study, the highest total amount of biophenols was foundin samples obtained from the early ripening (I) stage using the Ultrasound method compared with samples obtained from the same period using the Cm. Specifically, there was a strong decrease in biophenol content in the samples obtained using the Ultrasound method from the early ripening (I) stage to the late ripening (II) stage: 900.8 mg/kg ± 10.3 mg/kg and 571.9 mg/kg ± 9.9 mg/kg, respectively. Thus, the Ultrasound method had a higher capacity for biophenol extraction for both ripening stages (I and II). Among the secoiridois, the highest level of oleacein was found in the early ripening (I) stage using the Ultrasound method compared with the Cm: 345.5 mg/kg ± 26.9 mg/kg and 163.8 mg/kg ± 22.5 mg/kg, respectively. The highest amount of oleocanthal was found in the samples from the early ripening (I) stage obtained using the Us method: 90.5 mg/kg ± 5.9 mg/kg.

3.4. Multivariate statistical analysis of major components of EVOO samples (^{1}H ZG, BUCKET-1)

The NMR technique has been widely used with multivariate analysis (MVA) to differentiate EVOO samples according to cultivar and/or geographical origin (Girelli, Del Coco, Papadia, De Pascali, & Fanizzi, 2016; Girelli et al., 2018). In the present study, the analysis focused essentially on the harvest time and the differences in the extraction process. All the ^{1}H NMR spectra, acquired with the ZG sequence and giving the bucket-reduced dataset BUCKET-1, showed the characteristic signals of saturated (SFA), monounsaturated fatty acids (MUFA) and polyunsaturated (PUFA) fatty acids for the samples of EVOO obtained using by Ultrasound and Cm extraction processes (Fig. 1S). An explorative PCA model was obtained, with the corresponding t[1]/t[2] PCA score plot: $R^2X = 0.81$, $Q^2 = 0.74$, $P < 0.05$ (Fig. 3aS). The results

Table 2
Mean ± SD values for oil quality indexes (acidity, peroxide value, UV absorption and ethyl esters) and total phenolic content for EVOOs obtained by ultrasound (Us) and traditional (Cm) extraction process in the different ripening stages, and for each considered municipality (province of Bari). Values of tyrosol, hydroxytytrosol, oleacein, oleocanthal, lignans, aglycone oleuropein/ligstroside and total biophenols are expressed as mg/kg of oil (I, November; II, January).

Miller	I. Cm Giovinazzo	I. Us Giovinazzo	II. Cm Sannicandro	II. Us Sannicandro
acidity (% m/m oleic acid)	0.10 ± 0.03	0.11 ± 003	0.35 ± 0.03	0.23 ± 0.03
peroxide value (meq O_2/kg)	1.7 ± 0.22	1.7 ± 0.22	4.0 ± 0.22	3.1 ± 0.22
K232 (nm)	1.57 ± 0.043	1.74 ± 0.043	1.62 ± 0.043	1.60 ± 0.043
K268 (nm)	0.18 ± 0.014	0.22 ± 0.014	0.16 ± 0.014	0.17 ± 0.014
Delta K	0.004	0.005	0.004	0.005
hydroxytyrosol (3.4-DHPEA)	2.5 ± 0.1	0.7 ± 0.1	1.0 ± 0.1	1.3 ± 0.1
tyrosol (*p*-HPEA)	3.7 ± 0.9	1.2 ± 0.4	1.9 ± 0.5	1.7 ± 0.3
oleacein (3.4-DHPEA-EDA)	163.8 ± 22.5	345.5 ± 26.9	75.7 ± 23.5	127.0 ± 27.1
oleocanthal (*p*-HPEA-EDA)	76.7 ± 6.2	90.5 ± 5.9	42.7 ± 7.7	69.2 ± 4.9
lignans	162.9 ± 11.7	198.3 ± 15.2	120.5 ± 13.5	130.6 ± 16.4
aglycone oleuropein (3.4-DHPEA-EA)	102.3 ± 10.3	109.3 ± 12.4	66.1 ± 10.7	91.2 ± 8.7
aglycone ligstroside (*p*-HPEA-EA)	133.2 ± 13.7	155.3 ± 11.5	132.9 ± 16.1	150.9 ± 11.7
total biophenols	645.1 ± 9.3	900.8 ± 10.3	440.8 ± 10.4	571.9 ± 9.9

Miller	I, Cm Giovinazzo	I, Us Giovinazzo	II, Cm Sannicandro	II, Us Sannicandro
acidity (% m/m oleic acid)	0.10	0.11	0.35	0.23
peroxide value (meq O_2/kg)	1.7	1.7	4.0	3.1
K232 (nm)	1.57	1.74	1.62	1.60
K268 (nm)	0.18	0.22	0.16	0.17
Delta K	0.004	0.005	0.004	0.005
hydroxytyrosol (3,4-DHPEA)	2.5	0.7	1.0	1.3
tyrosol (*p*-HPEA)	3.7	1.2	1.9	1.7
oleacein (3,4-DHPEA-EDA)	163.8	345.5	75.7	127.0
oleocanthal (*p*-HPEA-EDA)	76.7	90.5	42.7	69.2
lignans	162.9	198.3	120.5	130.6
aglycone oleuropein (3,4-DHPEA-EA)	102.3	109.3	66.1	91.2
aglycone ligstroside (*p*-HPEA-EA)	133.2	155.3	132.9	150.9
total biophenols	645.1	900.8	440.8	571.9

showed that there was a clear separation of samples according to the harvesting time and based essentially on differences in the SFA and PUFA contents. In particular, from the corresponding loadings plot of the PCA model (Fig. 3bS), a high relative content of SFA (loading 1.26 ppm) was observed for both Cm and Ultrasound EVOOs obtained in the early (I) ripening stage. However, a high relative amount of PUFA, such as linoleic acid and linolenic acid at loadings of 0.9, 1.3, 2.02 and 5.34 ppm, was found in the EVOOs obtained using both the Cm and the Ultrasound method from the late ripening (II) stage. The observed differences could be due to the variations in the oil biosynthesis during the different harvesting stages. Although the amounts of SFA and PUFA (i.e. linoleic and linolenic) may depend on the time of harvest (Beltrán, del Rio, Sánchez, & Martínez, 2004), the amount of MUFA (i.e. mainly oleic acid) varies with the crop year and is strictly cultivar dependent. Studies have also demonstrated that the levels of SFA, such as palmitic acid, and PUFA decrease and increase, respectively, with fruit ripening (Baccouri et al., 2008). Interestingly, the PCA analysis of the bucket-reduced ^{1}H NMR spectra, acquired with only the ZG sequence (BUCKET-1), showed a negligible differentiation between samples from the early ripening (I) stage according to the extraction process used. However, there were clear differences in the samples from the late ripening (II) stage according to the extraction process used (i.e. Ultrasound method or Cm).

3.5. Multivariate statistical analysis minor components of EVOO samples (^{1}H NOESYGPPS, BUCKET-2)

MVA was also applied to the selected NMR dataset resulting from presaturation experiments and enhancing only the unsaponifiable fraction signals of samples of EVOO from the bucket-reduced spectra in the 10.00–5.50 ppm region (BUCKET-2). The aldehydic and aromatic regions of the NMR spectrum of olive oil were characterized by resonances ascribable to phenolic compounds, mainly tyrosol and hydroxytyrosol derivatives and their aldehydic forms in the spectral range 6.80–6.50 ppm and to aldehydes in the spectral range 9.70–9.20 ppm (Fig. 1S). It should be noted that free tyrosol and hydroxytyrosol were usually found in very low levels in EVOOs, although several well-known esterified derivatives of these compounds were present (Ruiz-Aracama, Goicoechea, & Guillén, 2017). In particular, these NMR signals (in the range 6.80–6.76 ppm) may include the dialdehydic form of decarboxymethyl elenolic acid esterified with tyrosol, which is also called oleocanthal or *p*-HPEA-EDA, the monoaldehydic form of ligstroside aglycone, which is also called *p*-HPEA-EA, the dialdehydic form of decarboxymethyl elenolic acid linked to hydroxytyrosol, which is also called oleacein or 3,4-DHPEA-EDA and the monoaldehydic forms of oleuropein aglycone (3,4-DHPEA-EA) (Ruiz-Aracama, Goicoechea, & Guillén, 2017). Oleocanthal also showed unbiased NMR signals in the spectral range 9.24–9.20 ppm, while the oleacein resonance was observed in the region between 9.66 and 9.62 ppm, which partially overlapped the oleocanthal and elenolic acid related signals. For ligstroside (*p*-HPEA-EA) and oleuropein aglycone (3,4-DHPEA-EA), unbiased NMR signals in the range 9.54–9.48 ppm were also identified (Del Coco, De Pascali, & Fanizzi, 2014; Ruiz-Aracama, Goicoechea, & Guillén, 2017).

The MVA focused on the possible differences in the minor components of EVOO samples collected during the two different harvesting stages. Interestingly, the PCA performed on the data revealed a clear difference in the EVOO samples collected according to the harvesting stage and the extraction process used (Fig. 4S). This oil sample distribution was confirmed by the corresponding OPLS-DA statistical model score plot shown in Fig. 1A. The OPLS-DA model showed a clear difference between the EVOO samples obtained using the Cm and the Us method: $P < 0.05$, $R^2X = 0.92$, $R^2Y = 0.92$, $Q^2 = 0.83$, p[CV-ANOVA] = 1.13*10–15. The loadings analysis shown in the S-line plot for the OPLS-DA model (Fig. 1B), revealed that there was a higher relative content of phenolic compounds, such as tyrosol and hydroxytyrosol derivatives in the Us- Coratina EVOO samples (loadings in the spectral range 6.80–6.70 ppm and 6.62–6.56 ppm). The presence of a high relative content of the dialdehyde oleocanthal (*p*-HPEA-EDA) which characterized Ultrasound compared to Cm samples was confirmed by the corresponding loadings in the spectral range 9.66–9.62 and 9.24–9.20 ppm for aldehydic protons in C-3 and C-1, respectively. Nevertheless, the spectral ranges 9.66–9.62 ppm, in which the C-3 aldehydic proton of *p*-HPEA-EDA was found, also contained the NMR signals for oleacein (aldehydic proton C-1) and elenolic acid, giving a complex pattern (Ruiz-Aracama, Goicoechea, & Guillén, 2017). However, the EVOO obtained by the Cm process was characterized by a high relative content of formaldehyde, with loadings in the spectral region 8.12–8.08 ppm (Ruiz-Aracama, Goicoechea, & Guillén, 2017), which is normally present in pungent oils, such as Coratina (Brescia & Sacco, 2008).

The OPLS-DA model was also built for the bucket-reduced dataset of

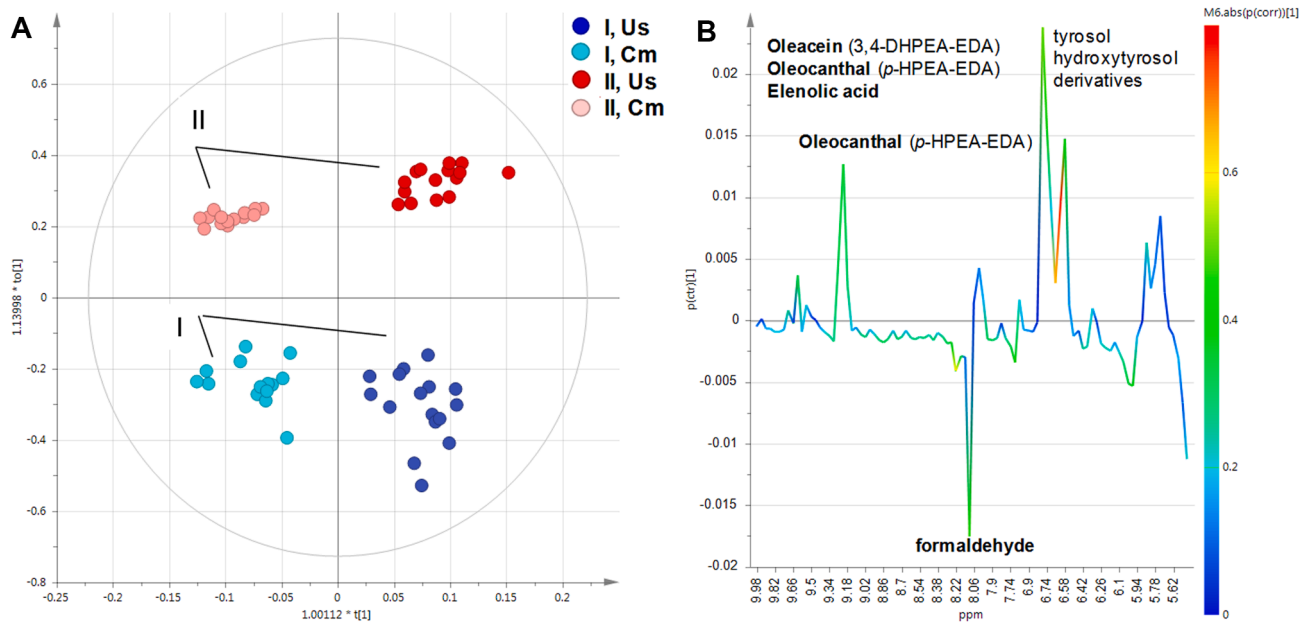

Fig. 1. **(A)** OPLS-DA score plot ($R^2X = 0.92$, $R^2Y = 0.92$, $Q^2 = 0.83$p[CV-ANOVA] $= 1.13*10^{-15}$) and **(B)** the corresponding S-line plot for the minor components model displaying the discriminant metabolites and the related predictive loadings (Variables obtained from the ^{1}H NMR spectra are coloured according to the correlation scaled loading (p(corr)). I and II indicated the first (November) and the last (January) harvesting period, respectively. (Cm = traditional; Us = ultrasound-assisted extraction process). The outer ellipse represents the 95% confidence interval (T^2 Hotelling).

the major components (BUCKET-1), using conventional (Cm) and Ultrasound method as class membership (Fig. 5S). The two OPLS-DA models, which were obtained from the datasets for the major and minor components (BUCKET-1 and BUCKET-2), were evaluated by comparing the Q^2 predictivity parameter. From this analysis, it was evident that both models were acceptable with a slight increase in the Q^2 value for the dataset related to EVOOs minor ($Q^2 = 0.83$, Fig. 1) compared with the major components ($Q^2 = 0.60$, Fig. 5S). However, it should be noted that a reasonable separation among samples was evident in both the two models along the orthogonal component [1], with a greater value of R^2Y for the OPLS-DA obtained for minor components ($R^2Y = 0.92$) compared with the model for the major components ($R^2Y = 0.77$). Because the R^2Y value is the uncorrelated variation of data X (i.e., the bucket-reduced NMR dataset) to data Y (i.e., the class membership or, in this case, the ltrasound method versus the conventional), the results confirmed the cluster separations according to the ripening stage and the PCA.

The marked intra-class gap of the samples from the OPLS-DA score plot is illustrated in Fig. 1. The intra-class gap was mainly due to differences between the early ripening (I) stage and the late ripening (II) stage. In other words, the EVOOs from the early ripening stage were clearly different from the samples obtained from the late ripening stage, especially along the second component to[1], for samples obtained using the Cm and Us method. Therefore, in order to analyze the differences between the extraction processes, a further investigation was performed that considered the early ripening and late ripening stages separately. A supervised (OPLS-DA) MVA demonstrated that the samples from Cm and Ultrasound methods were separated along the t[1] predictive component of the scoreplots (Fig. 2A, C). The statistical analysis demonstrated good OPLS-DA models ($P < 0.05$), with one predictive and two orthogonal components for the early (I) and late (II) ripening stage, respectively ($R^2X = 0.73$, $R^2Y = 0.98$, $Q^2 = 0.97$, p[CV-ANOVA] $= 1.51*10^{-16}$ and $R^2X = 0.64$, $R^2Y = 0.99$, $Q^2 = 0.98$, p[CV-ANOVA] $= 9.25*10^{-20}$). Specifically, the EVOO samples obtained using the Cm and the Us method from the late ripening (II) stage were more separated from each other when compared with the Cm and Ultrasound samples collected during the early ripening (I) stage. Therefore, the different extraction processes appear to be more effective in producing marked differences in samples collected during the late ripening stage compared with samples from the early ripening stage (Fig. 2A, C). The loading analysis (S-line plots) obtained from the OPLS-DA models (Fig. 2B, D), showed that several NMR signals could be used to discriminate the samples obtained using the Ultrasound method from the samples obtained using the Cm. For both ripening stages (I and II), the Ultrasound samples were characterized by a higher relative content of phenolic compounds, such as tyrosol and hydroxytyrosol derivatives oleocanthal and oleacein. Interestingly, there were significant differences between Cm and Us samples of olives collected in the late ripening (II) stage compared with samples collected during the early ripening (I) stage. It should be noted that tyrosol and hydroxytyrosol moieties, with NMR signals in the range 6.80–6.76 ppm, belonging to their esterified derivatives are substantially the most indicative among the phenolic compounds present in a high quality EVVO (Del Coco, De Pascali, & Fanizzi, 2014; Ruiz-Aracama, Goicoechea, & Guillén, 2017), such as Coratina based EVOO (Del Coco, De Pascali, & Fanizzi, 2014). This result was extremely important when we considered the differences between the minor components in the EVOO samples obtained using the Cm and the Us method. As shown by the MVA, the OPLS-DA models obtained for the early ripening (I) and late ripening (II) stages (Fig. 2A and 2C, respectively) were compared with the corresponding OPLS-DA model of the major components (Fig. 3A and 3C, respectively). A poor separation was found for samples from the early ripening stage (Fig. 3A), and there was a low Q^2 value for the dataset related to the major components of the EVOO samples ($Q^2 = 0.36$). There was a relevant scattering of samples on both the predictive t[1] and the orthogonal to[1] components for the early ripening samples (I), which confirmed the whole data OPLS-DA results of Fig. 5S. As a consequence, the discriminant metabolite S-line plot of the corresponding Fig. 3B indicated there were only slight differences in MUFA content, such as oleic acid (Girelli, Del Coco, Papadia, De Pascali, & Fanizzi, 2016). Conversely, the OPLS-DA model for the late ripening stage (Fig. 3C and D) showed a good clustering of samples according to the extraction processes used (i.e., the Cm and the Us method), as well as an improvement in the Q^2 value (model predictive capability). The discriminating variables responsible for this separation were principally related to the high relative content of PUFA in the samples obtained using the Cm and the high content of

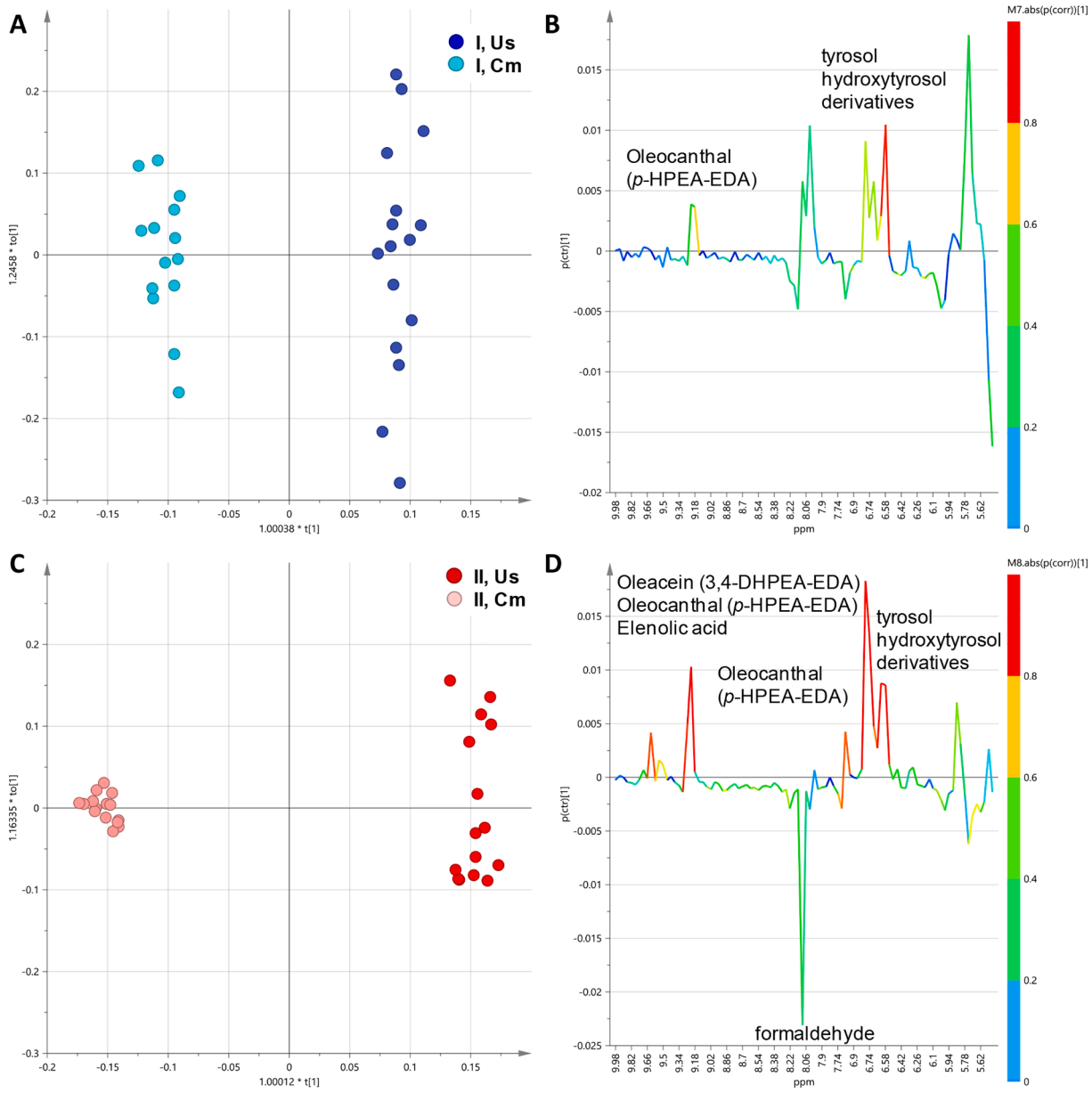

Fig. 2. (A, C) OPLS-DA score plots obtained for minor components fraction, for the early (I) and the last (II) ripening stage, respectively. (B, D) The corresponding S-line plots for each statistical model, displaying the discriminant metabolites and the related predictive loadings (Variables obtained from the ^{1}H NMR spectra are coloured according to the correlation scaled loading (p(corr)). (Cm = traditional; Us = ultrasound-assisted extraction process).

MUFA, such as oleic acid, obtained using the Us method. Moreover, considering the model's predictive ability (Q^2) for each harvesting stage, it is evident that the minor components were clearly differentiated in the Ultrasound extracted Coratina samples even in the early ripening stage. Indeed the Q^2 parameter dramatically increased from the early to late ripening stage when the major components were considered: $Q^2 = 0.36$ and $Q^2 = 0.91$ or the early and late ripening stages, respectively; the Q^2 parameter was also consistently higher for the early and late ripening stages for the minor components: $Q^2 = 0.97$ and $Q^2 = 0.98$, respectively.

3.6. Identification of metabolites and determination of fold changes

The significant variations shown in the MVA for the discriminant metabolite content obtained by the Ultrasound method and the Cm were evaluated using univariate analysis. For this purpose, a manual integration of the relevant NMR signals based on the internal standard (TMS) and the related fold changes (FCs) was obtained. Significant FCs were obtained by ^{1}H NMR peaks areas with a minimum $P < 0.05$ for oleacein, aglycone oleuropein (chemical shift 9.54 ppm), ligstroside oleuropein (chemical shift 9.50 ppm), olecanthal (chemical shift 9.22 ppm) and tyrosol/hydroxytyrosol derivatives (chemical shift 6.78 ppm). These values were compared with the oil quality parameters shown in Table 2. We found that, for both ripening stages (I and II), the discriminating molecule content increased in Us when compared with Cm samples (Fig. 4). The MVA showed that the discriminant metabolites in samples obtained during the early ripening (I) stage were the total biophenols and oleocanthal (see Fig. 2A); oleacein, aglycone, and ligstroside oleuropein, and oleocanthal FCs were found to be significant in the late ripening (II) stage. The obtained variations were similar in several cases, particularly for the total biophenol evaluation, which suggested a possible use of the NMR technique for this specific purpose (Olmo-Cunillera, López-Yerena, Lozano-Castellón, Tresserra-Rimbau, Vallverdú-Queralt, & Pérez, 2019).

Finally, to evaluate the relationship between ripeness and minor

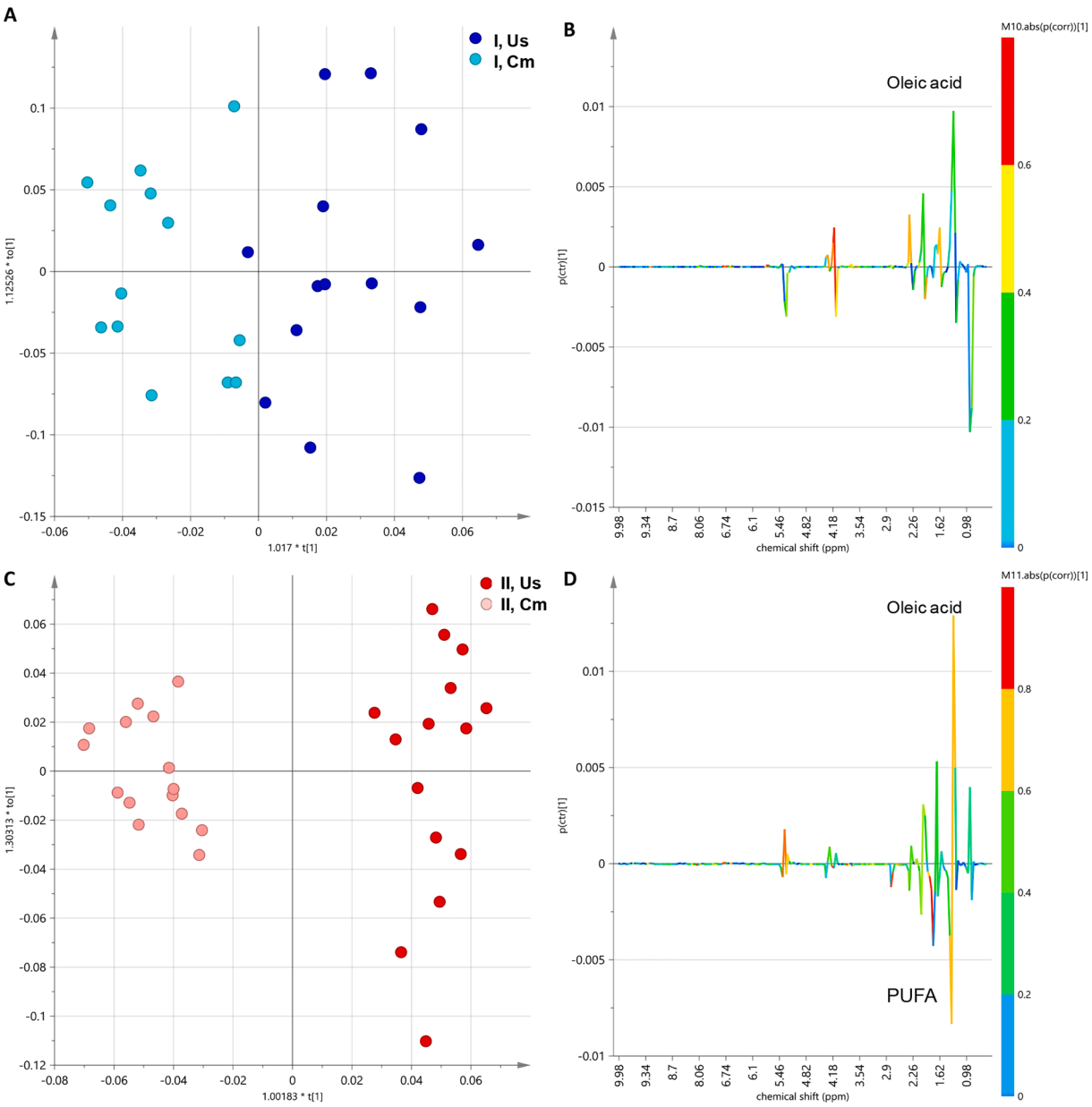

Fig. 3. (A, C) OPLS-DA score plots obtained for major components fraction, for the early (I) and the last (II) ripening stage, respectively. **(B, D)** The corresponding S-line plots for each statistical model, displaying the discriminant metabolites and the related predictive loadings (Variables obtained from the ^{1}H NMR spectra are coloured according to the correlation scaled loading (p(corr)). (Cm = traditional; Us = ultrasound-assisted extraction process).

component variations, the EVOO samples obtained using the Us method from the early and late ripening stages were considered. Although Coratina EVOO has been constantly reported to contain significant concentrations of phenolic compounds (Deiana, Santona, Dettori, Culeddu, Dore, & Molinu, 2019), high levels of tyrosol/hydroxytyrosol secoiridoid derivatives were found in the ripening stages. In particular, as shown in the PCA score plot (Fig. 6S) the early (November) and the late (January) ripening stage resulted clearly separated. From the discriminant loadings of the PCA model, it is possible to highlight the metabolites responsible for the observed differences. Particularly, the NMR signals corresponding to tyrosol/hydroxytyrosol derivatives (chemical shift 6.78 ppm), hydroperoxides (chemical shift 5.74 ppm), total oleacein, oleocanthal and elenolic acid (chemical shifts of 9.62 ppm), and oleocanthal (chemical shift 9.22 ppm) were identified from previous studies (Alexandri, Ahmed, Siddiqui, Choudhary, Tsiafoulis, & Gerothanassis, 2017; Ruiz-Aracama, Goicoechea, & Guillén, 2017).

4. Discussion

The Apulia region is covered with cultivated olive trees. This ancient crop has created the presence of synonyms and homonyms, as well as the formation of clonal populations. Molecular markers have become important tools to distinguish and characterize olive trees (D'Agostino et al., 2018). In particular, the SSR markers, which are versatile, informative, and widely distributed throughout the genome, currently represent the primary tool for investigating the genetic variation in olive germplasm (Pasqualone, Di Rienzo, Nasti, Blanco, Gomes, & Montemurro, 2013). In this study, a complete genetic identity of all samples with the Coratina profile was provided, which supported the importance of olive tree genotyping. The quality parameters of all the analyzed samples complied with the limits set by the European Union for EVOO values (Baiano, Gambacorta, Terracone, Previtali, Lamacchia, & La Notte, 2009; Gambacorta, Faccia, Previtali, Pati, Notte, & Baiano, 2010). Moreover, the NMR-based metabolomic approach (MVA) applied

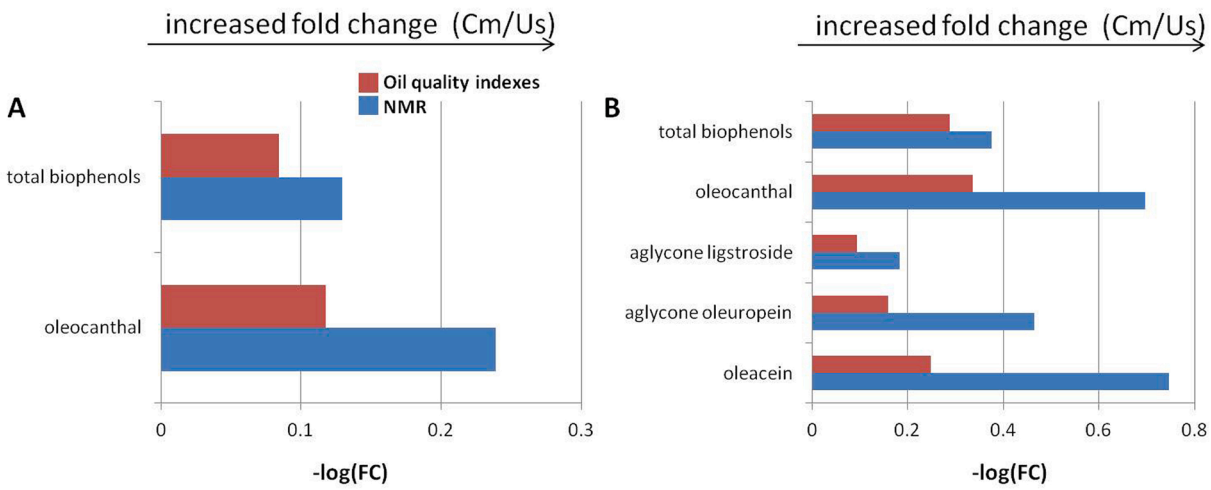

Fig. 4. (A) November, early and (B) January, late ripening stage Log2 fold change (FC) ratio for normalized bucket intensities, obtained by NMR-MVA, in Us (sonicated) with respect to Cm (traditional extraction process) EVOOs, in comparison with with oil quality indexes.

to both the major and minor components of EVOOs allowed us to analyze the differences between olive oil extracted using the Us method and the Cm, as well as between olives harvested during the early ripening (I) and the late ripening (II) stages. The results from this study were highly consistent with the total phenolic content analyses carried out according to the analytical methods described in Regulation EEC/2568/91. A very high content of phenolic compounds was found in samples from the early ripening stage (900.8 ± 10.3 mg/kg for total biophenol content; 1.2 ± 0.4 and 0.7 ± 0.1 mg/kg for tyrosol and hydroxytyrosol, respectively). However, a lower amount of total biophenols was detected in the samples from the late ripening (II) stage. Other studies have reported on the losses of phenolic compounds that occur with ripening, which are attributed to enzymatic hydrolysis (Gambacorta, Faccia, Previtali, Pati, Notte, & Baiano, 2010). Among the considered olive cultivars, the highest phenolic decrease during ripening and storage was found for Coratina olive oil, strongly correlated with its antioxidants content (Baiano, Gambacorta, Terracone, Previtali, Lamacchia, & La Notte, 2009). Moreover, for oleocanthal, the measured values obtained by classical analytical methods agreed with the MVA of the NMR data for the early ripening (I) and the late ripening (II) stages: 90.5 ± 5.9 and 69.2 ± 4.9 mg/kg, respectively. Thus, the high oleocanthal values in samples from the early ripening stage were significantly reduced in samples from the late ripening stage. As reported by other investigators (Deiana, Santona, Dettori, Culeddu, Dore, & Molinu, 2019), the levels of oleocanthal, oleacein and aglycon of oleuropein and ligstroside are strongly affected by the olive cultivar because these molecules decrease during the ripening process in all varieties, except for Coratina. Interestingly, the cumulative data obtained for EVOOs, which considered the extraction method used and the compositional trend at the different ripening stages, indicated the Ultrasound method had a clear advantage over the Cm. In addition to a higher intrinsic process yield, the Ultrasound method offers the possibility of benefitting from a relatively higher content of polyphenols at late ripening stages, which is generally associated with the highest oil yields. Finally, it should be noted (Table 2) that Ultrasound treatment results in a not uniform increase of all phenolic compounds. This may occur, because the final concentration of these molecules into the oil is the result of a complex combination of mechanical, biochemical (i.e. polyphenol oxidase and peroxidase activities) and chemical (distribution equilibria between the oily and aqueous phases) reactions influenced by the regulation conditions of the extraction process (specific energy, time, temperature and oxygen concentration in the atmosphere in contact with the olive paste).

5. Conclusions

The Ultrasound extraction process was used during the 2019/2020 harvesting campaign of Coratina EVOO in a homogeneous pedoclimatic area of Bari province (Italy); the area had the same environmental conditions and agronomic management. Two different olive ripening stages (early and late) were considered and the Us method was compared with Cm. Differences between the two extraction processes were observed using the NMR-based chemometric approach for the major and minor components of the complex matrices. High levels of biophenols, such as the tyrosol and hydroxytyrosol derivatives oleocanthal (*p*-HPEA-EDA), oleacein (3,4-DHPEA-EDA), elenolic acid and aglycone oleuropein (3,4-DHPEA-EA) and ligstroside (*p*-HPEA-EA) were found in the Coratina EVOO samples obtained using the Us method compared with the Cm. The observed differences were more marked in samples from the late ripening stage. Data obtained by the ^{1}H NMR and MVA clearly indicated that using the Us method increased the yield and the relative content of polyphenols. These findings also showed that NMR spectroscopy is a potent tool for the qualitative and quantitative analyses of EVOO. In particular, NMR fingerprinting provides snapshots of the overall molecular content present in the EVOO products. Thus, NMR can provide useful information for producers in order to help develop new extraction strategies for plant optimization and to increase the healthy bioactive product components in the EVOO products.

Funding

This work has been supported by the INNONETWORK PRIN-CORATINA (P8K5PA8) project “Processo Innovativo per la valorizzazione dell’olio extravergine di oliva monovarietale Coratina come nutraceutico nei processi infiammatori dell’intestino”.

CRediT authorship contribution statement

L. Del Coco: Investigation, Formal analysis, Validation, Writing - original draft. **C.R. Girelli:** Software, Data curation. **F. Angilè:** Data curation. **I. Mascio:** Resources. **C. Montemurro:** Resources, Formal analysis. **E. Distaso:** Formal analysis. **P. Tamburrano:** Formal analysis. **S. Chiurlia:** Formal analysis. **M.L. Clodoveo:** Resources, Validation. **F. Corbo:** Formal analysis. **R. Amirante:** Investigation, Validation. **F.P. Schena:** Conceptualization, Writing - review & editing, Funding acquisition. **F.P. Fanizzi:** Methodology, Writing - review & editing, Supervision.

Declaration of Competing Interest

The authors declare that they have no known competing financial interests or personal relationships that could have appeared to influence the work reported in this paper.

Acknowledgements

The authors give special thanks to olive oil suppliers "Olearia Pazienza, C.da Pianta di Rogadeo, 70032 Bitonto (Ba) Italy", "Giuseppe Vacca Olii S.r.l. - Bitonto 70032 (Ba) Italy" "Frantoio Mimi di Donato Conserva, Modugno (BA) Italy", DEOL of Eng C. De Palma, Bari, Italy and Pitagora of A. Manzulli, Taranto, Italy for the partnership .and collaboration.

Appendix A. Supplementary data

Supplementary data to this article can be found online at https://doi.org/10.1016/j.foodchem.2020.128778.

References

Alexandri, E., Ahmed, R., Siddiqui, H., Choudhary, M. I., Tsiafoulis, C. G., & Gerothanassis, I. P. (2017). High resolution NMR spectroscopy as a structural and analytical tool for unsaturated lipids in solution. *Molecules, 22*, 1663–1735. https://doi.org/10.3390/molecules22101663.

Amirante, R., & Clodoveo, M. L. (2017). Developments in the design and construction of continuous full-scale ultrasonic devices for the EVOO industry. *European Journal of Lipid Science and Technology, 119*, 1600438. https://doi.org/10.1002/ejlt.201600438.

Arafat, S. M., Abd-Elfatah, M. A., & Aml, M. T. (2020). New derivatives of phenolic compounds as index of olive oil quality. *Discovery, 56*, 26–35.

Baccouri, O., Guerfel, M., Baccouri, B., Cerretani, L., Bendini, A., & Lercker, G. (2008). Chemical composition and oxidative stability of Tunisian monovarietal virgin olive oils with regard to fruit ripening. *Food Chemistry, 109*, 743–754. https://doi.org/10.1016/j.foodchem.2008.01.034.

Baiano, A., Gambacorta, G., Terracone, C., Previtali, M., Lamacchia, C., & La Notte, E. (2009). Changes in phenolic content and antioxidant activity of Italian extra-virgin olive oils during storage. *Journal of Food Science, 74*, C177–C183. https://doi.org/10.1111/j.1750-3841.2009.01072.x.

Bellumori, M., Cecchi, L., Innocenti, M., Clodoveo, M. L., Corbo, F., & Mulinacci, N. (2019). The EFSA health claim on olive oil polyphenols: Acid hydrolysis validation and total hydroxytyrosol and tyrosol determination in Italian virgin olive oils. *Molecules, 24*(11), 2179–2195. https://doi.org/10.3390/molecules24112179.

Beltrán, G., del Rio, C., Sánchez, S., & Martínez, L. (2004). Influence of harvest date and crop yield on the fatty acid composition of virgin olive oils from cv. Picual. *Journal of Agricultural And Food Chemistry, 52*(11), 3434–3440. https://doi.org/10.1021/jf049894n.

Boucheffa, S., Miazzi, M. M., di Rienzo, V., Mangini, G., Fanelli, V., Tamendjari, A., … Montemurro, C. (2017). The coexistence of oleaster and traditional varieties affects genetic diversity and population structure in Algerian olive (Olea europaea) germplasm. *Genetic Resources and Crop Evolution, 64*(2), 379–390. https://doi.org/10.1007/s10722-016-0365-4.

Brescia, M. A., & Sacco, A. (2008). High-resolution ^{13}C nuclear magnetic resonance in the study of oils. In G. A. Webb (Ed.), *Modern magnetic resonance* (pp. 1637–1643). Dordrecht: Springer.

Bro, R., Kjeldahl, K., Smilde, A., & Kiers, H. (2008). Cross-validation of component models: A critical look at current methods. *Analytical and Bioanalytical Chemistry, 390*(5), 1241–1251. https://doi.org/10.1007/s00216-007-1790-1.

Carriero, F., Fontanazza, G., Cellini, F., & Giorio, G. (2002). Identification of simple sequence repeats (SSRs) in olive (*Olea europaea* L.). *Theoretical and Applied Genetics, 104*(2–3), 301–307. https://doi.org/10.1007/s001220100691.

Cipriani, G., Marrazzo, M., Marconi, R., Cimato, A., & Testolin, R. (2002). Microsatellite markers isolated in olive (*Olea europaea* L.) are suitable for individual fingerprinting and reveal polymorphism within ancient cultivars. *Theoretical and Applied Genetics, 104*(2–3), 223–228. https://doi.org/10.1007/s001220100685.

Clodoveo, M. L. (2019). Industrial ultrasound applications in the extra-virgin olive oil extraction process: History, approaches, and key questions. *Foods, 8*, 121–145. https://doi.org/10.3390/foods8040121.

Clodoveo, M. L., Camposeo, S., Amirante, R., Dugo, G., Cicero, N., & Boskou, D. (2015). Research and innovative approaches to obtain virgin olive oils with a higher level of bioactive constituents. In D. Boskou (Ed.), *Olive and olive oil bioactive constituents* (pp. 179–215). Elsevier Inc.. https://doi.org/10.1016/B978-1-63067-041-2.50013-6.

Clodoveo, M. L., Moramarco, V., Paduano, A., Sacchi, R., Di Palmo, T., & Crupi, P. (2017). Engineering design and prototype development of a full scale ultrasound system for virgin olive oil by means of numerical and experimental analysis. *Ultrasonics Sonochemistry, 37*, 169–181. https://doi.org/10.1016/j.ultsonch.2017.01.004.

Commission Implementing Regulation (EU) No 29/2012 of 13 January 2012 on marketing standards for olive oil. (Vol. 29/2012, pp. 3-10). Official Journal of the European Union. http://data.europa.eu/eli/reg_impl/2012/29/oj.

Commission Regulation (EEC) No 2568/91 of 11 July 1991 on the characteristics of olive oil and olive-residue oil and on the relevant methods of analysis. http://data.europa.eu/eli/reg/1991/2568/2015-10-16.

Conte, L., Bendini, A., Valli, E., Lucci, P., Moret, S., & Maquet, A. (2019). Olive oil quality and authenticity: A review of current EU legislation, standards, relevant methods of analyses, their drawbacks and recommendations for the future. *Trends in Food Science & Technology*. https://doi.org/10.1016/j.tifs.2019.02.025. In Press, Corrected Proof.

D'Agostino, N., Taranto, F., Camposeo, S., Mangini, G., Fanelli, V., Gadaleta, S., et al. (2018). GBS-derived SNP catalogue unveiled wide genetic variability and geographical relationships of Italian olive cultivars. *Scientific Reports, 8*(1). https://doi.org/10.1038/s41598-018-34207-y.

De la Rosa, R., James, C., & Tobutt, K. (2002). Isolation and characterization of polymorphic microsatellites in olive (*Olea europaea* L.) and their transferability to other genera in the Oleaceae. *Molecular Ecology Notes, 2*, 265–267. https://doi.org/10.1046/j.1471-8286.2002.00217.x.

Deiana, P., Santona, M., Dettori, S., Culeddu, N., Dore, A., & Molinu, M. G. (2019). Multivariate approach to assess the chemical composition of Italian virgin olive oils as a function of variety and harvest period. *Food Chemistry, 300*, Article 125243. https://doi.org/10.1016/j.foodchem.2019.125243.

Del Coco, L., De Pascali, S. A., & Fanizzi, F. P. (2014). ^{1}H NMR spectroscopy and multivariate analysis of monovarietal EVOOs as a tool for modulating Coratina-based blends. *Foods, 3*, 238–249. https://doi.org/10.3390/foods3020238.

Del Coco, L., Felline, S., Girelli, C. R., Angilè, F., Magliozzi, L., Almada, F., … Fanizzi, F. P. (2018). ^{1}H NMR Spectroscopy and MVA to evaluate the effects of caulerpin-based diet on *Diplodus sargus* lipid profiles. *Marine Drugs, 16*, 390–402. https://doi.org/10.3390/md16100390.

di Rienzo, V., Sion, S., Taranto, F., D'Agostino, N., Montemurro, C., & Fanelli, V. (2018). Genetic flow among olive populations within the Mediterranean basin. *PeerJ, 6*, Article e5260. https://doi.org/10.7717/peerj.5260.

European Commission Regulation 432/2012 establishing a list of permitted health claims made on foods, other than those referring to the reduction of disease risk and to children's development and health. (2012), (pp. L 136, 131−140): Official Journal of the European Communities. https://eur-lex.europa.eu/LexUriServ/LexUriServ.do?uri=OJ:L:2012:136:0001:0040:EN:PDF.

Gambacorta, G., Faccia, M., Previtali, M., Pati, S., Notte, E. L., & Baiano, A. (2010). Effects of olive maturation and stoning on quality indices and antioxidant content of extra virgin oils (cv. Coratina) during storage. *Journal of food science, 75*, C229–C235. https://doi.org/10.1111/j.1750-3841.2010.01516.x.

Girelli, C. R., Del Coco, L., & Fanizzi, F. P. (2017). Tunisian Extra Virgin Olive Oil Traceability in the EEC Market: Tunisian/Italian (Coratina) EVOOs Blend as a Case Study. *Sustainability, 9*, 1471–11050. https://doi.org/10.3390/su9081471.

Girelli, C. R., Del Coco, L., Papadia, P., De Pascali, S. A., & Fanizzi, F. P. (2016). Harvest year effects on Apulian EVOOs evaluated by ^{1}H NMR based metabolomics. *PeerJ, 4*, Article e2740. https://doi.org/10.7717/Peerj.2740.

Girelli, C. R., Del Coco, L., Zelasco, S., Salimonti, A., Conforti, F., & Biagianti, A. (2018). Traceability of "Tuscan PGI" extra virgin olive oils by ^{1}H NMR metabolic profiles collection and analysis. *Metabolites, 8*, 60–77. https://dx.doi.org/10.3390%2Fmetabo8040060.

Jerman Klen, T., & Mozetič Vodopivec, B. (2011). Ultrasonic extraction of phenols from olive mill wastewater: Comparison with conventional methods. *Journal of Agricultural and Food Chemistry, 59*(24), 12725–12731. https://doi.org/10.1021/jf202800n.

Olive Oil Times. (2020). Retrieved from: https://www.oliveoiltimes.com/business/olive-oil-production-in-italy-to-exceed-original-estimates/74380 Accessed 26/11/2020.

Olmo-Cunillera, A., López-Yerena, A., Lozano-Castellón, J., Tresserra-Rimbau, A., Vallverdú-Queralt, A., & Pérez, M. (2019). NMR spectroscopy: A powerful tool for the analysis of polyphenols in extra virgin olive oil. *Journal of the Science of Food and Agriculture, 100*, 1842–1851. https://doi.org/10.1002/jsfa.10173.

Pasqualone, A., Di Rienzo, V., Nasti, R., Blanco, A., Gomes, T., & Montemurro, C. (2013). Traceability of Italian protected designation of origin (PDO) table olives by means of microsatellite molecular markers. *Journal of Agricultural And Food Chemistry, 61*, 3068–3073. https://doi.org/10.1021/jf400014g.

Reboredo-Rodríguez, P., Varela-López, A., Forbes-Hernández, T. Y., Gasparrini, M., Afrin, S., & Cianciosi, D. (2018). Phenolic compounds isolated from olive oil as nutraceutical tools for the prevention and management of cancer and cardiovascular diseases. *International Journal Of Molecular Sciences, 19*, 2305–2326. https://doi.org/10.3390/ijms19082305.

Regulation, E. C. (2016). Reg. No. 2016/2095 Amending Regulation (EEC) No 2568/91. On the characteristics of olive oil and olive-residue oil and on the relevant methods of analysis. Official Journal of European Union, L326, 1. http://data.europa.eu/eli/reg_del/2016/2095/oj.

Ruiz-Aracama, A., Goicoechea, E., & Guillén, M. D. (2017). Direct study of minor extra-virgin olive oil components without any sample modification. ^{1}H NMR multisupression experiment: A powerful tool. *Food Chemistry, 228*, 301–314. https://doi.org/10.1016/j.foodchem.2017.02.009.

Sefc, K., Lopes, M., Mendonça, D., Santos, M. R. D., Machado, M. L. D. C., & Machado, A. D. C. (2000). Identification of microsatellite loci in olive (*Olea europaea*) and their characterization in Italian and Iberian olive trees. *Molecular Ecology, 9*, 1171–1173. https://doi.org/10.1046/j.1365-294x.2000.00954.x.

Sion, S., Taranto, F., Montemurro, C., Mangini, G., Camposeo, S., & Falco, V. (2019). Genetic characterization of apulian olive germplasm as potential source in new breeding programs. *Plants, 8*, 268–282. https://doi.org/10.3390/plants8080268.

Spadoni, A., Sion, S., Gadaleta, S., Savoia, M., Piarulli, L., & Fanelli, V. (2019). A simple and rapid method for genomic DNA extraction and microsatellite analysis in tree plants. *Journal of Agricultural Science and Technology, 21*, 1215–1226.

van den Berg, R. A., Hoefsloot, H. C., Westerhuis, J. A., Smilde, A. K., & van der Werf, M. J. (2006). Centering, scaling, and transformations: Improving the biological information content of metabolomics data. *BMC Genomics, 7*, 142–157. https://doi.org/10.1186/1471-2164-7-142.